

## SUPERPLASTICITY AND SUPERPLASTIC DEFORMATION MECHANISM OF A SiC<sub>p</sub>/2024Al COMPOSITE\*

Ying Yan      Boran Liu      Caibei Zhang

Box 104, College of Science, Northeastern University,  
Shenyang, Liaoning, 110006, P.R. China

**ABSTRACT** A highest elongation of 290% and a maximum  $m$  value of 0.49 were recorded at a strain rate of  $8.33 \times 10^{-4} \text{ s}^{-1}$  at 793K for an IM SiC<sub>p</sub>/2024Al composite. The equiaxed structure was observed at the initial stage of superplastic deformation. With increasing elongation, the sizes of grains gradually decreased and grain shape coefficient gradually increased. But during superplastic deformation, grains fundamentally remained equiaxed structure. At the moment of failure, grain shape coefficient increased to 1.58. This indicated that macroscopic deformation of the composite was not caused by the grain elongation, but mainly by the grain boundary sliding. Dislocation and an appropriate liquid phase at matrix-reinforcement interfaces and/or grain boundaries played a positive role to grain boundary sliding.

**Keywords:** *superplasticity, superplastic deformation mechanism, composite*

### 1. INTRODUCTION

Aluminum alloy matrix composites reinforced with discontinuous SiC particles have been one of the most attractive metal matrix composites on account of their good property and reasonable price. Now they have been extensively and deeply studied, and brought into applicable stage. However, their ductility is yet not good enough to do production with complex profiles, and thus restricts their applications. Superplastic forming is an available technique that is used to solve this problem. By using this technique, we can simplify processes and save materials in manufacturing<sup>[1]</sup>.

The composites produced by the powder metallurgy (PM) have very fine grains and fewer microstructure defects, so they exhibited high strain rate superplasticity<sup>[2,3]</sup>. But the composites manufactured by ingot metallurgy (IM) will play an increasingly more important role in the future applications because IM is of low cost in producing aluminum alloy matrix composites,

In the present paper, superplastic tensions on an IM SiC<sub>p</sub>/2024Al composite were carried out. In the meantime, its microstructure at the optimum superplastic condition and fracture surfaces at different temperatures were investigated, and the superplastic deformation mechanism at the optimum superplastic condition was discussed also.

---

\* The subject aided by National Nature Science Foundation Committee of China (Subject No. 59571006).

## 2. EXPERIMENTAL PROCEDURES

The composite used in this investigation was supplied by Shanghai Jiaotong University. The matrix metal is commercial 2024 Al alloy with weight percentage composition: 4.4 Cu, 1.5 Mg, 0.6 Mn, and 93.5Al, and the reinforced material is 15wt% SiC particulate with mean size  $14\mu\text{m}$ . The ingots were hot compressed from  $\Phi 100\text{mm}$  to  $\Phi 150\text{mm}$ . The purpose of hot compression is to improve their ductility and avoid cracking during rolling. After Al-covering, the plates were processed by hot rolling and cold rolling, and a thin plate with 1.2mm thick was obtained. Tensile specimens with a 6mm gage width and 10mm length were tested at temperatures ranging from 763K to 803K at strain rates from  $1.67 \times 10^{-4} \text{ s}^{-1}$  to  $1.67 \times 10^{-3} \text{ s}^{-1}$ . Microstructure of the composite was examined before, during and after testing by optical microscope and TEM. Fracture surfaces were observed by SEM.

## 3. RESULTS AND DISCUSSIONS

### 3.1 Superplasticity

Fig.1 shows the elongation to failure as a function of the initial strain rate at different temperatures. A highest elongation of 290% was obtained at  $8.33 \times 10^{-4} \text{ s}^{-1}$  at 793K. The range of the superplastic temperatures was about 783K~803K. This range was higher in comparison with 2024 Al alloy<sup>[4]</sup>. This occurred because superplastic deformation mechanism of 2024Al alloy is grain boundary sliding. If temperature increased, precipitates would dissolve and lose their effect of impeding grain growth. But in the composite, SiC particles could stabilize the grain sizes and a liquid phase at grain boundaries and/or SiC/Al interfaces could relax stress concentration caused by superplastic deformation. Fig.2 shows that the flow stress and strain rate curve at 793K. A maximum  $m$  value of 0.49 was obtained at  $8.33 \times 10^{-4} \text{ s}^{-1}$ . This value is lower than that of 2024 Al alloy, because the strength of irregular shape SiC particles is higher than that of the matrix alloy. SiC particles restricted the ductility flow of the matrix and caused the non-uniform deformation.

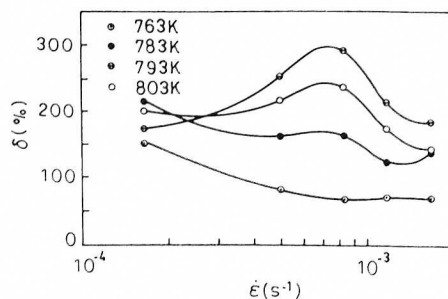


Figure 1. Relationship between elongation and initial strain rate at different temperatures

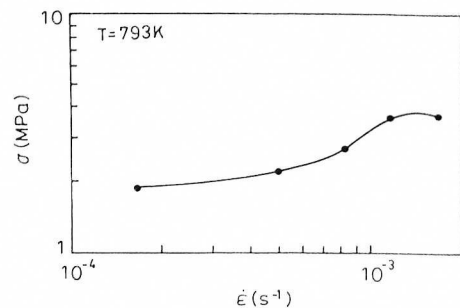


Figure 2. Flow stress as a function of strain rate at 793K

### 3.2 Microstructure

At the initial stage of superplastic deformation, the equiaxed structure was observed (see Fig.3 (a) ). With increasing elongation, the grain sizes gradually decreased and grain shape coefficients increased slowly. When elongation reached 200%, the grain sizes rapidly dropped and the shape coefficient increased to 1.27. In the meantime, the fine grains increased dramatically in number and their distributions were non-uniform very much (see Fig.3(b)). This took place because dynamic recrystallization occurred at some high stress concentration regions such as triple junctions at grain boundaries, SiC/Al interfaces, and so on. When specimen was failure, the shape coefficient reached 1.58. The increase of grain shape coefficients might be caused by the following reasons. With the increase of elongation, many grain boundary dislocations were produced, and the climb of grain boundary edge dislocations along boundaries would mainly occur in the transversal boundaries where it was accompanied by vacancy emission. Thus the vacancy concentration near transversal boundaries must be higher than that near boundaries with a different orientation with respect to the highest tensile strain axis<sup>[5]</sup>. Therefore, the migration rate of the transversal boundaries increased.

When grains were elongated along the tensile direction, triple junctions at boundaries changed from equilibrium state to non-equilibrium state. Thus grain boundary Gibbs free energy increased and thermodynamic driving force which inhibited the migration of transversal boundaries appeared and increased with the increase of elongation of grains. So the elongation of grains during superplastic deformation should come to an end upon attaining a definite degree of elongation. In the used composite, the maximum grain elongation degree was 1.58. This indicated that macroscopic deformation of the composite was not caused by grain elongation, but mainly by grain boundary sliding.

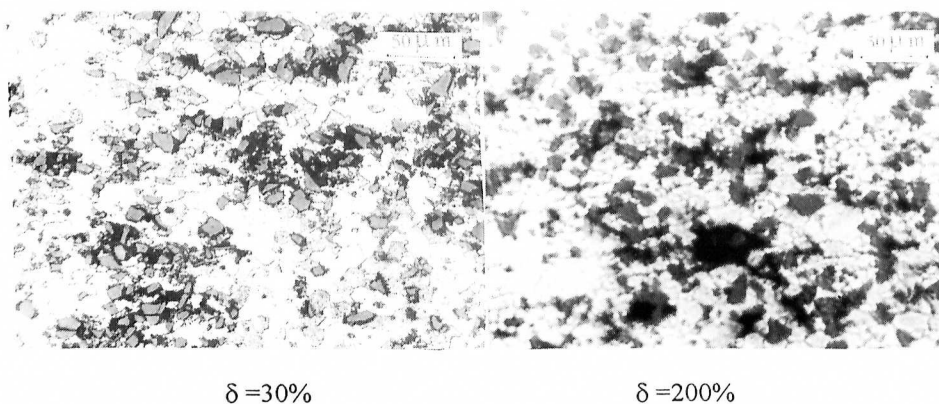


Figure 3. Optical microstructures of the SiC<sub>p</sub>/2024Al composite at different elongations at the optimum superplastic condition

### 3.3. Dislocation

When specimen was strained to  $\delta = 80\%$ , there was a reasonably low dislocation density and the dislocations intercrossed into nets each other (see Fig.4(a)). As the increase of elongation,

dislocation density and length increased, and they did not interact with each other (see Fig4(b)). And inside grains helical dislocations were formed by interaction of dislocations and vacancies. When elongation reached 200% (see Fig.4(c)), dislocations interacted to form tangled and cellular structure and density was corresponded to that of Fig.4 (b). The change of dislocation structure might be caused by dynamic recovery. And the increase of dislocation density indicated that dislocations played a positive role to promote grain boundary sliding in the process of superplastic deformation.

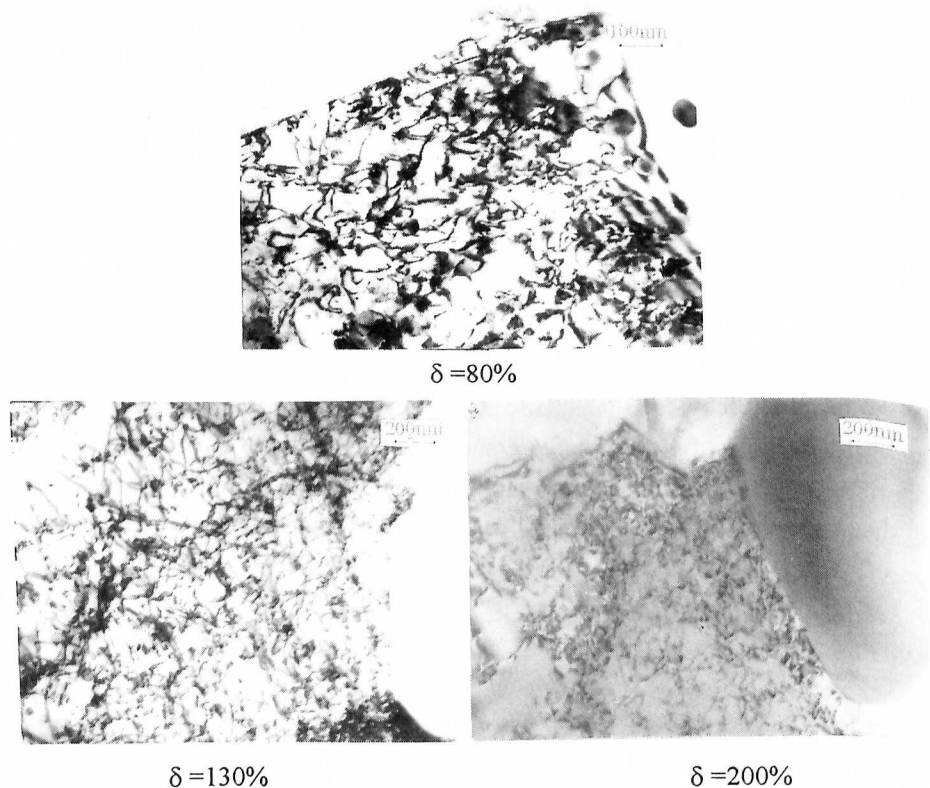


Figure 4. TEM of the composite at different elongations at the optimum superplastic condition

### 3.4. Fracture Surface

Figure 5 shows fracture surfaces at different temperatures. The fracture surface basically consisted of many dimples and cavities at 763K (see Fig.5(a)). Some metal whiskers with sub-micrometer in diameter and several  $\mu\text{m}$  in length could be seen at local rupture sites (see Fig5(b)). At 783K, local fracture surfaces still consisted of dimples and cavities, but most rupture sites consisted of linear bands which were almost parallel to tensile direction. The width of the bands was about  $3\sim 10\mu\text{m}$ . Every band contained many fine bands with a spacing of less than  $2\mu\text{m}$ . Simultaneously, thin and short whiskers were formed directly from some fine bands (see Fig5(c)). When temperature reached 793K, the fracture surface was covered by wavy flow lines and showed a messy appearance. Many whiskers with length about  $20\sim 60\mu\text{m}$  were formed from the flow lines covering the rupture surface (see Fig5(d)).

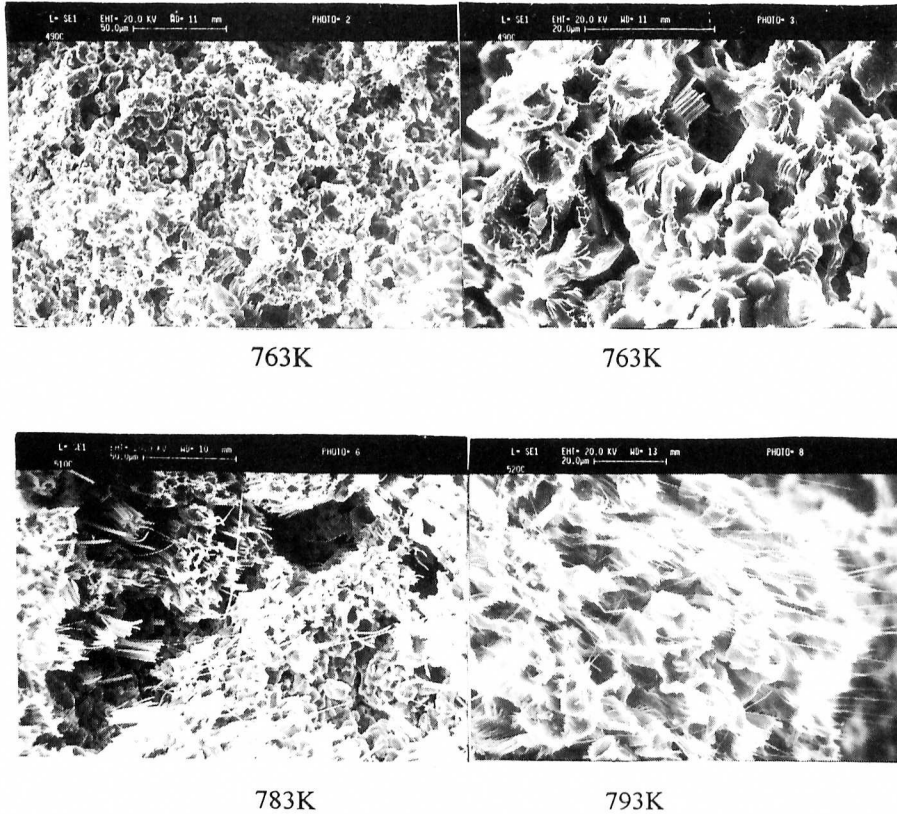


Figure 5. Fracture surfaces of the SiC<sub>p</sub>/2024Al composite at different temperatures

Jae-Hong Kim et al<sup>[6]</sup> thought that the strength  $\sigma_c$  of the composite with the fiber volume fraction  $V_f$  is approximated by:

$$\sigma_c = (1 - V_f) \sigma_m + V_f \dot{\epsilon} \eta L^2 / (Dh)$$

where  $\sigma_m$ ,  $\eta$ ,  $L$ ,  $D$ , and  $h$  are the strength of matrix, viscosity, the length of SiC fiber, the diameter of SiC fiber, and the thickness of the slurry layer, respectively. Slightly above the solidus temperature liquid, more precisely, slurry of both solid and liquid phase coexistence was preferentially formed at the SiC/Al interfaces or grain boundaries due to Mg and Cu segregation<sup>[7,8]</sup>. If solid and liquid coexisted in the form of slurry, the viscosity increased steeply with increasing solid fraction. At 783K, the slurry had sufficient rigidity to support its own weight, so linear bands were formed. At 793K, amount of the liquid phase at slurry layer increased, the value of  $\eta$  reduced and that of  $h$  increased, the slurry may lose the ability to support its own weight, thus wavy flow lines were formed. If the liquid phase at the slurry layer went on increasing,  $\sigma_c$  should reduce, grain boundaries hence lost the ability to transfer load from matrix to SiC particles, so elongation dropped. In the composite, when temperature increased to 803K, the maximum elongation dropped to 230% at  $8.33 \times 10^{-4} \text{ s}^{-1}$ . This

suggested that the appropriate liquid phase at the slurry layer could relax stress concentration during superplastic deformation and a much larger volume fraction of a liquid phase does not contribute to large elongation. It was probably associated with intragranular decohesion at the liquid grain boundaries. On the basis of W. P. Cao et al<sup>[9]</sup> investigations, the formation of metal whiskers was due to the intensive grain boundary sliding only within period immediately before or during the time when the specimen of undergoing superplastic deformation fractured. This suggested that grain boundary sliding might also be liquid-like viscous flow.

#### 4. Conclusions

1. The maximum elongation of 290% and  $m$  value of 0.49 in an IM 15wt% SiC<sub>p</sub>/2024Al composite, which was simply processed by hot rolling and cold rolling, were obtained at  $8.33 \times 10^{-4} \text{ s}^{-1}$  at 793K.

2. During superplastic deformation, grains basically remained equiaxed structure, dislocation density increased and structure changed from crossed nets form to tangled and cellular form.

3. When deformation temperatures were near or above the solidus temperature, grain boundary sliding behaved liquid-like viscous flow. Many metal whiskers were formed at the moment of fracture and its length and density increased as the increase of deformation temperatures.

4. Superplastic flow in an IM SiC<sub>p</sub>/2024Al composite which was in a roll state at the optimum superplastic condition was mainly controlled by a grain boundary sliding mechanism accommodated by intragranular sliding and an appropriate liquid phase at SiC<sub>p</sub>/Al interfaces and/or grain boundaries.

#### References

- [1] M. W. Mahoney, A. K. Ghosh and C. C. Bampton, in ICCM6 & ECCM2, Vol.2 (1987), pp.2372-2381, edited by F. L. Matthews, N. C. R. Buskell, J. M. Hodgkinson and J. Morton, London.
- [2] T. G. Nieh, J. Wadsworth and T. Imai, *Scripta Metall. Mater.*, 26 (1992), 703.
- [3] T. G. Nieh and J. Wadsworth, *Mater. Sci. Eng.*, A147 (1991), 129.
- [4] HUANG Hailing, The Thesis of M.S., Northeastern University, 12(1986).
- [5] M. Kh. RABINOVICH and V. G. TRIFONOV, *Acta Mater.*, 44 (1996), 2073.
- [6] Jae-Kong Kim, Dong Nyung Lee and Kyu Hwan Oh, *Scripta Metall. Mater.*, 29 (1993), 377.
- [7] S. R. Nutt and R. W. Carpenter, *Mater. Sci. Eng.*, 75 (1985), 169.
- [8] M. Strangwood, C. A. Hipsley and J. J. Lewandowski, *Scripta Metall. Mater.*, 24 (1990), 1483.
- [9] W. D. CAO, X. P. LU and H. CONRAD, *Acta Mater.*, 44 (1996), 697.